Contemporary Mathematics
https://ojs.wiserpub.com/index.php/CM/

Research Article

Mathematical Modeling and μ-Synthesis-Based Robust Control of Boost DC-DC Converters Using MATLAB

Nikolay Hinov[1*], Bogdan Gilev[2]

[1] Department of Computer Systems, Faculty of Computer Systems and Technologies, Technical University of Sofia, 8, Kliment Ohridski Blvd, Sofia, 1000, Bulgaria
[2] Department of Mathematics and Computer Science, University of Transport "Todor Kableshkov", Sofia, 1574, Bulgaria
E-mail: hinov@tu-sofia.bg

Received: 12 July 2025; **Revised:** 8 September 2025; **Accepted:** 18 September 2025

Abstract: This paper presents a robust control framework for Boost Direct Current to Direct Current (DC-DC) converters based on μ-synthesis in MATLAB. The approach explicitly models structured parameter uncertainties, including the capacitor Equivalent Series Resistance (ESR) and load variations, and tailors the weighting filters to balance tracking performance, control effort, and noise attenuation. In simulations, the μ-controller achieves zero overshoot, settling time $\approx$ 1.2 ms, and steady-state error $<$ 0.01 V, while a tuned Proportional-Integral-Derivative (PID) baseline exhibits ~12% overshoot, settling time $\approx$ 2.5 ms, and $\approx$ 0.45 V steady-state error under the same uncertainty set. Robust stability is certified by μ-bounds below unity across the design frequency band, and robust performance margins meet the specification. Novelty and contributions: explicit inclusion of capacitor ESR as a structured uncertainty in the modeling and synthesis loop; an implementation-oriented workflow (linearization $\rightarrow$ weighting design $\rightarrow$ D-K iteration $\rightarrow$ realization) with reproducible MATLAB code; and a quantitative benchmark versus a classical PID baseline under identical operating scenarios. The results support the deployment of the proposed controller in renewable and automotive applications that require resilience to parameter variations and fast transients.

***Keywords*:** Boost Direct Current to Direct Current (DC-DC) converter, robust control, μ-synthesis, MATLAB, mathematical modeling, state-space, linearization, power electronics

MSC: 93B51, 93C10, 93D09

1. Introduction

Direct Current to Direct Current (DC-DC) converters are widely used in modern electronic systems where efficient conversion and control of electrical energy is required. One of the most common types is the Boost DC-DC converter, which converts the input voltage to a higher level. This class of converters finds applications in electric vehicles, renewable energy sources such as photovoltaic panels and wind turbines, industrial and domestic power supplies, and other systems where efficient power management is essential [1, 2].

The control of Boost DC-DC converters is challenging due to their nonlinear nature, load variations, changes in input voltage and circuit element values, and dynamic load transitions over wide ranges. Classical control methods, such as

DOI: https://doi.org/10.37256/cm.7120267821

Proportional-Integral-Derivative (PID) controllers, often do not provide sufficient robustness under dynamic conditions or in the presence of uncertainties and disturbances [3, 4]. In this context, robust control is a powerful tool for designing systems that maintain their stability and performance even under parameter uncertainty and external influences [5–7].

MATLAB provides an integrated environment for the analysis, modeling, and synthesis of control systems, including robust control. Techniques such as H_∞ control, μ-synthesis, Linear-Quadratic-Regulator (LQR) control, and adaptive methods have been successfully used to improve the stability and dynamic response of DC-DC converters [8, 9].

Robust control in power electronics focuses on the development of control systems that can maintain optimal device performance despite the presence of external disturbances and internal parameter changes [10]. This approach involves the application of modern control theories that use complex mathematical models to analyze and design controllers capable of compensating for possible system defects [11].

Robust control synthesis is a key approach for designing devices and systems that can maintain their stability and efficiency in the presence of uncertainties and disturbances. In order to make an appropriate choice of control synthesis method, the most popular robust control methods used in DC-DC converters are compared below, and their advantages, disadvantages and applicability will be indicated [12].

1.1 H_∞ control

H_∞ control is a powerful robust control method that is used to design control systems capable of providing good performance in the presence of uncertainties, disturbances, and variations in system parameters [13]. The main objective of H_∞ control is to minimize the worst-case control error by formulating the problem as an optimization problem. The main features of the method are that it uses the H_∞ norm to evaluate the performance and weighting functions to shape the frequency characteristics. Its advantages are: good performance over a wide range of disturbances and variations in circuit parameters; guaranteed stability for predefined uncertainty limits; global optimization, as it minimizes the maximum error over the entire frequency range; better dynamic response to transients compared to classical PID control; it can be combined with other control synthesis methods such as LQR, Fuzzy Logic, and Model Predictive Control (MPC), and also allows easy modeling and simulation in MATLAB [14]. The method is also characterized by the following disadvantages: Complex to set up and parameterize, because it requires complex mathematical calculations and system modeling, which in real-time operation requires fast processors such as Digital Signal Processor (DSP) and Field-Programmable Gate Array (FPGA); not always optimal-In some cases LQR or adaptive methods can give better results; requires precisely defined weighting functions. Ultimately, H_∞ control is a powerful method for robust control of power electronic devices and systems. Its application in DC-DC converters, grid inverters and electric motor control improves the stability, robustness and dynamics of control in the presence of disturbances and uncertainties [14, 15]. Thus, despite its complexity, H_∞ control is an effective tool for designing stable and reliable power electronic systems.

1.2 μ-synthesis

μ-synthesis is an extension of H_∞ control that additionally takes into account structured uncertainties in the system [16]. While H_∞ control ensures robust stability under uncertain external disturbances, μ-synthesis optimizes the control over dynamic variations in the system parameters. The method uses a Structured Singular Value (SSV), denoted by μ, to assess how uncertainties in the system affect stability and performance. The main goal of μ-synthesis of control is to minimize the maximum error amplification and ensure robust stability by solving an optimization problem. In this context, μ-synthesis is an iterative process that consists of the following main stages: H_∞ optimization-finding the best controller for given uncertainties; μ-Analysis-checking the stability through the structured singular value and updating the uncertainties and repeating the process [17]. The advantages of this method are: more efficient in models with large parameter uncertainties, because it treats not only external disturbances, but also internal changes in parameters; provides a better balance between robustness and performance; optimal behavior under uncertainties, because it reduces the worst effects of structured variations; has better performance than H_∞ control when parameters vary widely and supports automatic adaptation of the control to real conditions. Its disadvantages are: Computationally more complex than H_∞, because it applies more complex computational modeling and therefore requires more parameters for uncertainty

analysis; higher computational costs, because it requires powerful processors (DSP, FPGA) for real-time implementation; requires more in-depth knowledge of uncertainty modeling techniques and more difficult tuning because it uses more simulations and tests compared to standard H_∞ control [18].

μ-synthesis provides very good robustness in controlling complex power electronic systems. This makes it extremely suitable for: DC-DC converters with unknown and changing parameters, such as highly variable loads; inverters and grid converters subject to grid variations; control of electric motors and drives requiring stable control under different regimes; wireless power transmission systems where transmission conditions change dynamically [18]. Thus, despite the higher complexity, μ-synthesis is a powerful tool for creating extremely stable and efficient control systems in power electronics.

1.3 *LQR/Linear-Quadratic Gaussian (LQG)*

The LQR controller and the LQG controller are optimal control methods based on the theory of linear quadratic optimization problems [19]. They are used to design efficient controllers that minimize a given quadratic cost function, taking into account the dynamics of the system. LQR/LQG is particularly useful in power electronics because: it guarantees stability under changes in the load and system parameters; it optimizes the control dynamics by minimizing errors and control efforts. It is also applicable to linear and quasi-linear systems, being used in inverters, motors, converters, and others. Essentially, it is an optimal control method that minimizes the quadratic error function and the input signal of systems described by linear matrix state equations. LQG is an extension of LQR that includes a Kalman filter for control in the presence of noise and uncertainties [20]. LQG uses a Kalman Filter to estimate the state of the system in the presence of noise, and an LQR controller that uses this estimate for control. Thus, LQG is useful in power electronic systems where there are unmeasured states or noise in the measurements, such as in inverters, motors, and grid systems. The advantages of the method are as follows: it provides optimal system behavior by reducing errors and providing smooth dynamics; maintains stability under load changes; provides good energy efficiency by reducing losses and thermal loads; is easier to tune compared to H_∞ and μ-synthesis, and in addition, LQG works under noisy measurements and is thus useful in real-world applications such as transportation, energy, and industry [21]. Disadvantages of this approach are: it requires an accurate mathematical model, since if the system dynamics are not well described, the control does not work effectively; can be more complex to implement compared to PID or even H_∞ control; not the best choice for nonlinear systems, because LQR/LQG works best for linear or quasi-linear systems; has less robustness to large uncertainties and is more sensitive to noise modeling. LQR and LQG are optimal control methods that offer stability, fast response and efficiency in power electronics. They are used in power electronic converters, where the balance between control and power consumption is critical [22]. They are especially useful in: DC-DC converters (Buck, Boost) to maintain a stable voltage; inverters to reduce harmonic distortion; electric motor drives to implement better vector control; grid-tied systems for synchronization and improved Power Factor Correction (PFC) [23].

1.4 *Sliding-Mode Control (SMC)*

Sliding Mode Control is a nonlinear control method that provides robustness, fast dynamics, and resistance to variations in system parameters and external disturbances [24]. Essentially, it is a method for controlling nonlinear systems that provides high resistance to uncertainties through a switching control law, where the system is forced to follow a certain sliding surface. SMC is extremely popular in power electronics because: it provides stability under changes in load and voltage; it does not depend strongly on the accuracy of the mathematical model used; and it is resistant to external disturbances and variations in parameters. The main idea of SMC is to define a sliding surface $S(x)$ such that the system dynamics are always forced to follow this surface, regardless of disturbances and uncertainties in the circuit parameters [25]. The SMC controller usually consists of two main parts: a discontinuous controller (Switching Control), which forces the system to move towards the sliding surface, using switching laws such as a sign function for this purpose, and an Equivalent Control, which keeps the system on the sliding surface by applying a sliding condition (a condition for stability of the sliding mode). The advantages of the method are: robustness-it works well with variations in circuit parameters and external disturbances; fast dynamics, as the response to changes is faster compared to PID and LQR; effective in controlling nonlinear systems such as DC-DC converters and inverters; reduces the influence of

noise, which is very useful in powerful power electronic systems with industrial applications and in transportation [26]. Disadvantages of this approach are as follows: Chattering Effect, this is a high-frequency switching, which can lead to losses and electromagnetic interference; complexity in implementation, because it requires more complex algorithms for real-time operation; need for additional filtering, as techniques such as Boundary Layer or Super-Twisting Control must be used to reduce the chattering effect; can cause additional losses in powerful power electronic systems. SMC is a powerful nonlinear control method that provides robustness and fast dynamics in controlling power electronic devices. It finds application in: DC-DC converters, where it provides stability under dynamic loads; grid inverters-to reduce harmonic distortion; electric drives for improved speed and torque control of various types of electric motors; Wireless charging of energy storage elements for optimization of transmitted power [27, 28].

The choice of robust control method depends on the specific characteristics of the converter and the operating environment. H_∞ control is suitable for systems with known disturbances, μ-synthesis offers better performance with unknown parameters, LQR is a good balance between efficiency and energy optimization, while Sliding Mode Control is the most robust choice for nonlinear systems [29–32]. Table 1 provides a summary comparison of robust control synthesis methods with applications in power electronics.

Table 1. Comparison of the advantages and disadvantages of robust control synthesis methods with application in power electronics

Method	Uncertainty robustness	Ease of design	Computational complexity	Perturbation performance	Applicability
H_∞	High	Medium	High	High	Converters with known interference
μ-synthesis	Very high	Low	Very high	High	Systems with uncertain parameters
LQR/LQG	Medium	High	Medium	Medium	Optimized converters
SMC	Very high	Medium	Low	Very high	Nonlinear converters

H_∞ control guarantees robust performance for unstructured disturbances but does not directly model structured parametric variations. SMC provides strong robustness for nonlinear plants but may induce chattering and higher switching stress unless carefully mitigated. Adaptive/AI methods (fuzzy, Reinforcement Learning (RL) and MPC) offer adaptability but lack formal margins unless combined with robust designs. In contrast, μ-synthesis explicitly handles structured uncertainties (here: load R and capacitor Equivalent Series Resistance (ESR) R_C) via the structured singular value, providing formal robustness certificates and competitive controller order suitable for real-time implementation. This makes μ-synthesis the most appropriate choice for the present application.

This article will discuss the synthesis of a robust control for a DC-DC boost converter using MATLAB (μ-Synthesis). The dynamic model of the converter, its characteristics and limitations, and the application of modern control strategies will be analyzed. The presented simulations and analyses will demonstrate the advantages of robust control over traditional methods, focusing on the efficiency, stability, and adaptability of the system. MATLAB offers a comprehensive development environment that facilitates the synthesis, analysis, and verification of these methods. Through the built-in tools for automatic synthesis and optimization, MATLAB allows for fast and efficient finding of a robust controller that works in all possible scenarios. Instead of manually designing controllers through trial and error, MATLAB allows for: automated optimization of the control law to minimize errors and energy losses; testing multiple scenarios for the system dynamics through simulations; using robust synthesis algorithms that ensure stability even under unexpected changes in the converter parameters. This significantly reduces development time, providing more reliable and efficient results compared to traditional methods.

On the other hand, after successful design and verification, the controller must be implemented on hardware. MATLAB offers Embedded Coder and Hardware-in-the-Loop (HIL) simulations, which facilitate the implementation of algorithms in DSP, FPGA or microcontrollers (STM32, Texas Instruments C2000, etc.). This makes the transition from simulation to a real system much faster and more reliable. Ultimately, the above can be summarized as follows: MATLAB

is an indispensable tool for the synthesis of robust control of power electronic converters, as it provides automated control synthesis methods, powerful simulations and easy integration with real devices; robust methods designed in MATLAB guarantee high converter resilience to disturbances, load variations and input voltage changes; simulations reduce the time for experimental testing, providing reliable results before the controller is implemented in a real system; The ability to automatically generate code makes MATLAB an ideal platform for developing industrial and research applications in power electronics. Thus, using MATLAB for the synthesis of robust control of Boost DC-DC converters is critical to achieving reliability, efficiency, and rapid implementation in real applications. It is such a demonstration, based on a specific example of a nonlinear system, that is the motivation for writing this work.

1.5 *Contributions*

This work advances the application of μ-synthesis to boost converter control under structured uncertainties through the following contributions:

• Structured uncertainty modeling-derived from actual component tolerance data, covering variations in inductance, capacitance, and load resistance.

• Application-driven weighting function design-tailored to simultaneously enhance transient performance, limit steady-state ripple, and avoid actuator saturation.

• Scenario-based robustness validation-performed under realistic operating conditions relevant to electric vehicles and smart grid integration, ensuring stable performance across varying load and input conditions.

• Implementation-oriented control design-includes controller order reduction using balanced truncation, enabling practical deployment with negligible performance degradation.

These aspects distinguish the present study from conventional μ-synthesis applications, where weighting function selection and uncertainty modeling are often generic.

2. Synthesis in MATLAB of a robust controller providing current mode control of a Boost DC-DC converter

In this chapter, the task is to synthesize a robust control that provides the desired operating mode (current mode control) of a Boost DC-DC converter, i.e., a control that successfully maintains the operating mode when the model parameters (input voltage, output current and circuit variations) change within certain limits.

To solve the problem, the μ-Synthesis method was used [33–35].

2.1 *Synthesis of the mathematical model of the DC-DC converter*

The first step in the control synthesis is the process of linearization of the model. In this specific example, a Boost DC-DC converter will be used. The task is to synthesize a robust control using the linearized model, which will achieve stabilization of the desired current in the load circuit.

For this purpose, the basic mathematical model of the Boost DC-DC converter, which was synthesized with idealized circuit components, will be modified. Figure 1 shows the circuit of the DC-DC converter, with its active resistance-R_C added sequentially to the filter capacitor. This resistance describes the internal resistance of the filter capacitor. From data from manufacturers, it has been established that when the operating temperature of the device changes in the interval [−40 °C; +45 °C], this resistance changes in the interval [0.5 Ω; 5 Ω].

Usually, in most models, the internal resistance of the filter capacitor is neglected, but in the current mod control scheme, even a small change in this resistance can significantly degrade the performance of the controller. This requires a more in-depth study of the influence of this parameter, in order to develop a robust control of the DC-DC converter.

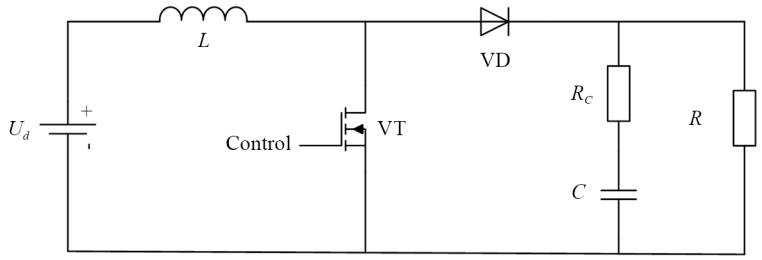

Figure 1. Boost DC-DC converter with addition of the active resistance of the filter capacitor

For the purposes of the study, an input voltage U_d = 10 V was selected and the following values of the circuit elements were determined: filter inductance L = 10e-6 H, filter capacitor C = 40e-6 F, active resistance of the filter capacitor R_C = 1 Ω, load resistance R = 50 Ω, with a range of variation in the interval $R \in [10\ \Omega;\ 50\ \Omega]$.

A continuous current operating mode was selected, with the switching frequency and the duty cycle being f = 400,000 Hz, D = 69%, respectively.

The DC-DC converter is described by a system of ordinary differential equations regarding the state variables. Switching functions are used to describe the different states of the power circuit, which are obtained as a result of the switching of the semiconductor switches. In the specific example, the following systems are obtained:

$$\begin{cases} L\dfrac{di_L}{dt} == U_d - \text{contr.}(u_C + i_C R_C) \\ i_R + i_C = \text{contr.} i_L \\ R_C i_C + u_C = R.i_R \\ C\dfrac{du_C}{dt} = i_C \end{cases} \quad \text{or} \quad \begin{cases} L\dfrac{di_L}{dt} == U_d - \text{contr.}(u_C + i_C R_C) \\ \dfrac{R_C i_C + u_C}{R} + i_C = \text{contr.} i_L \\ C\dfrac{du_C}{dt} = i_C \end{cases} \tag{1}$$

where the state variables are: i_L-the current through the inductance, u_C-the voltage on the filter capacitor;

After transformation, the final form of the model is obtained:

$$\begin{cases} L\dfrac{di_L}{dt} == U_d - \text{contr.}(u_C + i_C R_C) \\ (R_C + R) i_C = -u_C + \text{contr.} i_L.R \quad \text{for contr.} = \begin{cases} 1, & \text{for} \quad 0 < \text{rem}(t,\ T) \le D.T \\ 0, & \text{for} \quad D.T < \text{rem}(t,\ T) \le T \end{cases} \\ C\dfrac{du_C}{dt} = i_C \end{cases} \tag{2}$$

where contr is the function that implements the switching between the individual states of the DC-DC converter, D-duty cycle, $T = 1/f$-transistor switching period, and $\text{rem}(t,\ T)$-remainder of the division of t by T.

2.2 *Linearization of the model in a MATLAB/Simulink environment*

The linearization tool developed in MATLAB/Simulink calculates the matrices A, B, C and D of the linearized system describing the modeling object:

$$\begin{aligned} \dot{x} &= Ax + Bu \\ y &= Cx + Du \end{aligned} \tag{3}$$

where x-states space variable, u-input variable and u-output variable.

The matrices A, B, C and D are calculated so that the "behavior" of the nonlinear system and the linearized one are as "close" as possible. Different methods of linearization are used. The method used in this case is based on injecting unit signals at the input of the system and measuring the response of the outputs.

In order to linearize the DC-DC converter model, it is necessary to create a joint model of the power circuit with the controller, thus obtaining a generalized converter-PID controller, shown in Figure 2.

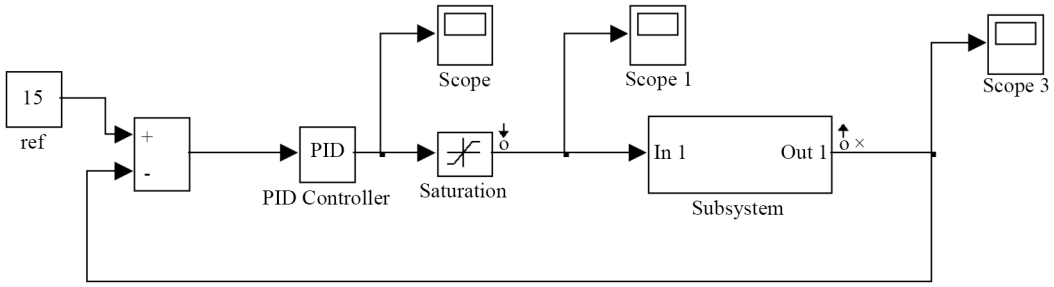

Figure 2. MATLAB/Simulink model of DC-DC converter in a form suitable for linearization

The content of the "Subsystem" block from Figure 2 is shown in Figure 3, it corresponds to the mathematical model of the power circuit of the DC-DC converter, described by (2).

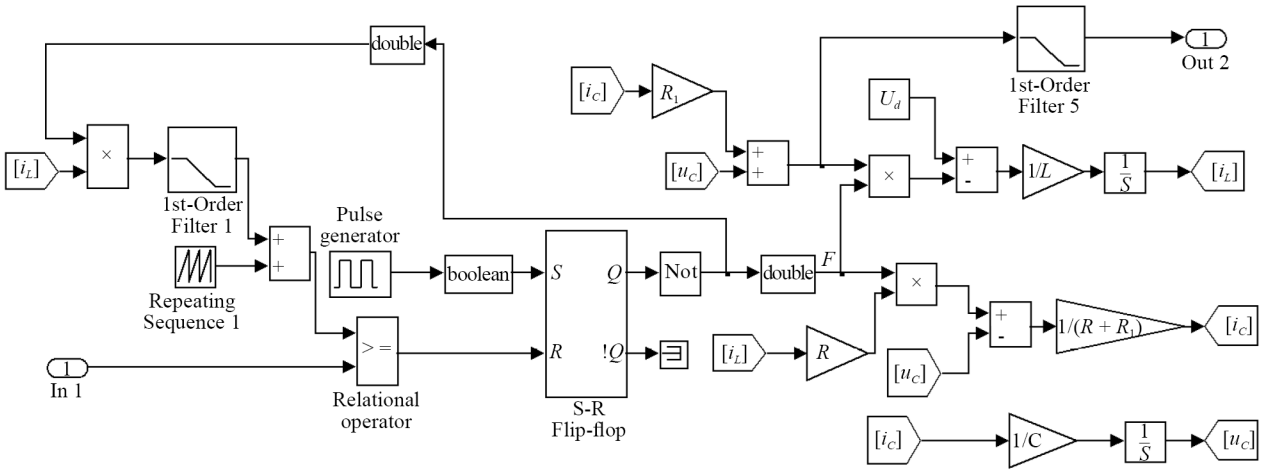

Figure 3. Contents of the "Subsystem" block from Figure 2

If we run the MATLAB/Simulink linearization tool on the model described in Figure 3, it will give an error. This is due to the fact that the "Subsystem" block contains non-smooth mathematical operations that describe the elements: trigger, pulse generator, etc. In order to implement a linearization procedure for a model in MATLAB/Simu, it is necessary to rework the relevant blocks so that they implement the "same" output, but do not use undesirable mathematical operations. For this purpose, the authors have developed an "equivalent" "Subsystem" block, the content of which is shown in Figure 4.

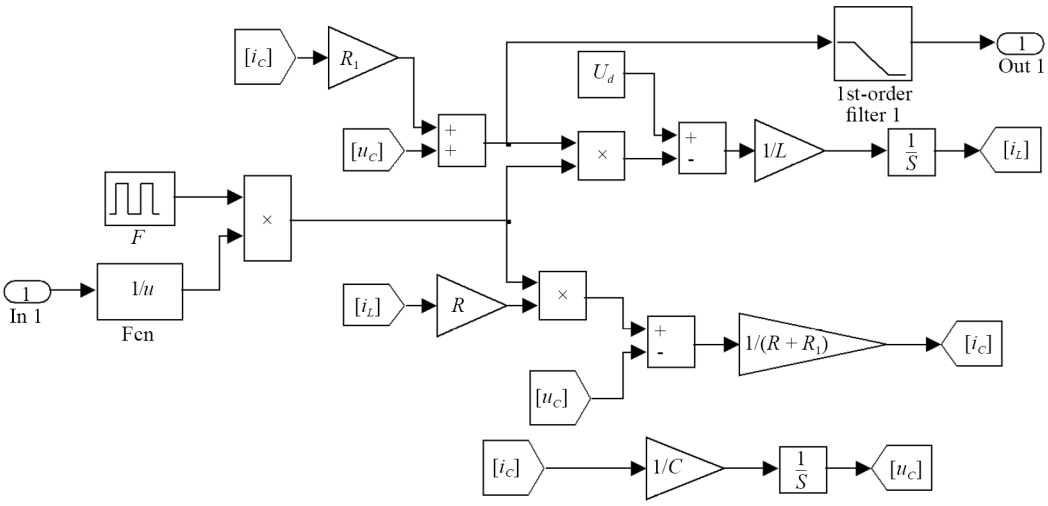

Figure 4. New content of the "Subsystem" block performing the same function as the "Subsystem" block from Figure 3

It is important to note that the "Subsystem" block in Figure 4 does not have a direct physical implementation, it simply performs the "same" function as the mathematical model of the converter.

The articles [36, 37] provide a detailed, step-by-step explanation of how to start the linearization tool in a MATLAB/Simulink environment, so this procedure will not be discussed in detail here. The difference is that in the above publications the model parameters are fixed at their nominal values, while in the case under consideration, limits are selected within which these parameters can be changed. These limits are as follows:

L = 10e-6 H-fixed at nominal value (without a limit of change, because it is assumed that it does not change relative to its nominal value);

C = 40e-6 F-fixed at nominal value (without a limit of change, because it is assumed that it does not change relative to its nominal value);

$R \in [10;\ 50]$ Ω-limits of change of the load resistance;

$R_C \in [0.5;\ 5]$ Ω-limits of variation of the active resistance of the filter capacitor.

For the thus selected limits of variation of the parameters, 4 linearization procedures were run, where the circuit parameters were selected as shown in Table 2.

Table 2. Linearization procedures for different values of L, C, R, and R_C

Procedure	L	C	R	R_C
1	10e-6	40e-6	10	0.5
2	10e-6	40e-6	10	5
3	10e-6	40e-6	50	0.5
4	10e-6	40e-6	50	5

After running the linearization tool, four different values were obtained for the matrices A, B, C, and D, corresponding to each of the 4 combinations of values of the circuit elements from Table 2. The values of these matrices thus obtained are presented in Table 3.

Table 3. Values for matrices A, B, C, and D for each of the four linearization procedures from Table 2

Procedure	A	B	C	D
1	$10^5\begin{pmatrix}-1 & 0 & 0\\ 0 & -0.4762 & -0.9524\\ 0 & 0.2381 & -0.0238\end{pmatrix}$	$10^6\begin{pmatrix}0\\ 1.4286\\ 0\end{pmatrix}$	$\begin{pmatrix}0 & 0 & 1\end{pmatrix}$	0
2	$10^5\begin{pmatrix}-1 & 0 & 0\\ 0 & -3.3333 & -0.6667\\ 0 & 0.1667 & -0.0167\end{pmatrix}$	$10^6\begin{pmatrix}0\\ 1\\ 0\end{pmatrix}$	$\begin{pmatrix}0 & 0 & 1\end{pmatrix}$	0
3	$10^5\begin{pmatrix}-1 & 0 & 0\\ 0 & -0.4950 & -0.9901\\ 0 & 0.2475 & -0.0050\end{pmatrix}$	$10^6\begin{pmatrix}0\\ 1.4851\\ 0\end{pmatrix}$	$\begin{pmatrix}0 & 0 & 1\end{pmatrix}$	0
4	$10^5\begin{pmatrix}-1 & 0 & 0\\ 0 & -4.5455 & -0.9901\\ 0 & 0.2273 & -0.0045\end{pmatrix}$	$10^6\begin{pmatrix}0\\ 1.3636\\ 0\end{pmatrix}$	$\begin{pmatrix}0 & 0 & 1\end{pmatrix}$	0

From the analysis of the data in Table 3, it is found that in matrices A and B only part of their elements change, while matrices C and D do not change. In summary, for the individual ones, we obtain the following:

$$A = 10^5\begin{pmatrix}-1 & 0 & 0\\ 0 & -1.9142 \pm 1.4191 & -0.8284 \pm 0.1617\\ 0 & 0.2071 \pm 0.0404 & -0.0141 \pm 0.0096\end{pmatrix}$$
$$B = 10^6\begin{pmatrix}0\\ 1.2425 \pm 0.2426\\ 0\end{pmatrix},\ C = \begin{pmatrix}0 & 0 & 1\end{pmatrix} \text{ and } D = 0 \tag{4}$$

Thus, the uncertain model of the DC-DC converter studies, taking into account uncertainties in the circuit parameters, is:

$$\left|\begin{array}{l}\begin{pmatrix}\dot{x}_1\\ \dot{x}_2\\ \dot{x}_3\end{pmatrix} = A\begin{pmatrix}x_1\\ x_2\\ x_3\end{pmatrix} + Bu,\\ y = x_3\end{array}\right. \tag{5}$$

where the matrices A and B with undefined elements are given by (4).

In a MATLAB environment using the code

```
% Uncertain model of a converter
a22 = ureal('a22', -1.9142, 'PlusMinus', 1.4191);
```

a23 = ureal('a23', -0.8284, 'PlusMinus', 0.1617);
a32 = ureal('a32', 0.2071, 'PlusMinus', 0.0404);
a33 = ureal('a33', -0.0141, 'PlusMinus', 0.0404);
A = 1e + 5*[-1, 0, 0; 0, a22, a23; 0, a32, a33];
b2 = ureal('b2', 1.2425, 'PlusMinus', 0.2426);
B = 1e + 6*[0; b2; 0];
C = [0, 0, 1];
D = 0;
G = uss(A, B, C, D).

An object G is generated that models a linear system with uncertainty, and in Matlab this is described by the following class:

Uncertain continuous-time state-space model with 1 outputs, 1 inputs, 3 states.
The model uncertainty consists of the following blocks:
a22: Uncertain real, nominal = -1.91, variability = [-1.42, 1.42], 1 occurrences
a23: Uncertain real, nominal = -0.828, variability = [-0.162, 0.162], 1 occurrences
a32: Uncertain real, nominal = 0.207, variability = [-0.0404, 0.0404], 1 occurrences
a33: Uncertain real, nominal = -0.0141, variability = [-0.0404, 0.0404], 1 occurrences
b2: Uncertain real, nominal = 1.24, variability = [-0.243, 0.243], 1 occurrences.

In this case, the object G has a standard structure and for this it is most convenient to use the "uss" command, if the object G has a more complex (non-standard) structure, then the "sysic" command should be used.

While polytopic and Linear Parameter-Varying (LPV) descriptions enable richer operating-region coverage, they can substantially increase controller order and synthesis burden. Interval arithmetic may be overly conservative. We therefore adopt structured parametric uncertainties (R, R_C) using ureal/uss, which reflects component tolerances and keeps synthesis tractable while enabling μ-based robustness certification.

The controller is synthesized on a linearized model around the operating point and then validated on a full nonlinear Pulse Width Modulation (PWM) model. This workflow captures the essential small-signal dynamics while ensuring out-of-set nonlinear validation. Alternatives such as feedback linearization or fuzzy modeling can better capture strong nonlinearities, yet they either require precise model inversion or lack formal robustness margins. Our results indicate that the μ-controller synthesized on the linearized plant retains performance on the nonlinear model within the tested operating envelope.

2.3 μ-synthesis on assignment

At this point, we use the already synthesized uncertainty model G to synthesize a μ controller K_μ.

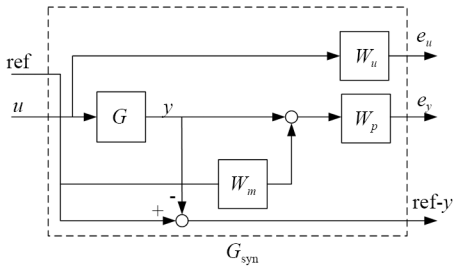

Figure 5. Structure of an extended open system G_{syn} used for synthesis of the controller K_μ

To synthesize this type of control, we use the extended open system G_{syn}, presented in Figure 5. This system is obtained by adding the filters W_p, W_u and W_m (as well as some additional connections) to the linearized uncertainty model G, and the extended open system G_{syn} is obtained.

Figure 5 shows the following basic blocks:

• filters scaling the input/output signals;

• reference model Wm implementing a transfer function (aperiodic unit) simulating the most favorable possible transient process;

• and the object G is obtained at the previous point.

The weighting functions were designed according to the following principles:

$W_p(s) = \dfrac{0.5s + 500}{s + 0.001}$-specifies the desired closed-loop bandwidth (~500 Hz) and attenuates switching noise beyond this frequency.

$W_u(s) = \dfrac{s + 50}{0.05s + 1}$-penalizes high-frequency control effort to avoid actuator saturation and excessive switching.

$W_m(s) = \dfrac{s + 5}{0.02s + 1}$-models sensor noise dynamics and measurement delay.

The selected weighting functions were validated by their frequency-domain characteristics, as shown in Figure 6. $W_p(s)$ provides high gain at low frequencies and a bandwidth of approximately 500 Hz, enabling effective disturbance rejection while attenuating high-frequency noise. $W_u(s)$ introduces a penalty on control effort to prevent actuator saturation and to minimize switching losses. $W_m(s)$ shapes the measurement noise and delay effects, enforcing low sensitivity in the high-frequency range. The magnitude profiles confirm that the weighting functions fulfill the design requirements for robustness and performance.

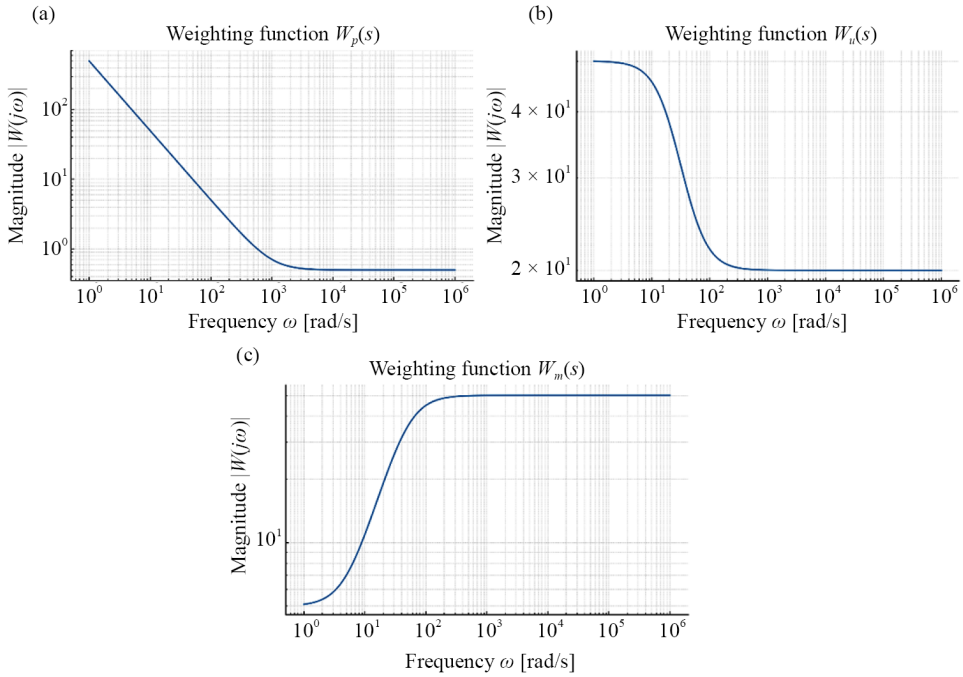

Figure 6. Bode magnitude plots of the selected weighting functions

We recall that the object is described by the system (2)-(3) and it has an input u and an output y, where y is the voltage on the load resistance, and u is the duty cycle D of the control pulses.

In the MATLAB environment, using the command, a structure of the open system G_{syn} is created with the following source code:

```
% filters
s = tf('s');
Wp = (s + 20000)/(s + 0.001);
```

```
Wu = 1e-2;
Wm = 1/(1e - 4 * s + 1);
% Open loop system -G_syn
systemnames = 'G Wm Wu Wp';
inputvar = '[ ref; control ]';
outputvar = '[ Wu; Wp; ref-G ]';
input_to_G = '[ control ]';
input_to_Wm = '[ ref ]';
input_to_Wu = '[ control ]';
input_to_Wp = '[ G-Wm ]';
G_syn = sysic.
```

The inputs of G_{syn} are ref and u, respectively, and the outputs are e_u, e_y and ref-y.

During μ-synthesis, the controller is searched for, for which the quality criterion is met.

As shown in [35], the task of obtaining robust controller quality is reduced to solving a problem of obtaining robust stability, in which the following function is required to be minimized:

$\mu_{\Delta_P}(F_l(G,\ K)(j\omega))$, for each $\bar{\sigma}(\Delta_P(j\omega)) < 1$, for each ω, where μ_{Δ_P} is the structural singular value, $\bar{\sigma}$ is the largest singular value of the corresponding transfer matrix, and $\Delta_P = diag(\Delta_F,\ \Delta)$ is the extended uncertainty, consisting of fictitious uncertainty Δ_F and parametric uncertainty Δ.

This classical μ-synthesis problem is solved by applying D-K iterations of the form:

$$\min_{K} \inf_{\widehat{D} \in D_{\Delta_P}} ||DF_L(G,\ K)D^{-1}||_{\infty}, \text{ for each } \max_{\omega} \bar{\sigma}(\Delta_P(j\omega)) \leq 1$$

where one of the two matrices $\widehat{D}$ or K is successively fixed and the other is minimized, and then vice versa.

In a MATLAB environment, using the dksyn command, the controller synthesis is implemented through D-K iterations, and thus the μ-controller K_μ is obtained. The synthesized μ-controller has order 5, corresponding to the two state variables of the boost converter augmented with the three weighting filters. After applying minimal realization, the order reduces to 4, which ensures a compact implementation without compromising robustness. To evaluate the performance of the synthesized controller, the output and input u of the Gsyn system are connected to the input and output of K_μ, respectively.

```
% Compute the Mu suboptimal controller
nmeas = 1;
ncont = 1;
fv = logspace(-3, 3,100);
opt = dkitopt('FrequencyVector', fv, ...
        'DisplayWhileAutoIter', 'off', ...
        'NumberOfAutoIterations', 3);
[k_mu, cls_mu, bnd_mu, dkinfo] = dksyn(G_syn, nmeas, ncont, opt).
```

In the case nmeas = 1 and ncont = 1, this indicates that a controller K_μ with one input and one output will be synthesized.

To test the behavior of the thus synthesized controller K_μ, the output ref-y and input u of the G_{syn} system are connected, respectively, to the input and output of the controller K_μ, and the clp_{syn} system is obtained, shown in Figure 7.

This connection is made with the so-called lower fractional-linear transformation $F_l(G_{\text{syn}},\ k_\mu)$, which is implemented programmatically with the lft command:

```
% Close loop system-clp_syn
clp_syn = lft(G_syn, k_mu, 1, 1).
```

The input of the newly obtained system clp_{syn} is ref, and the outputs are e_u and e_y.

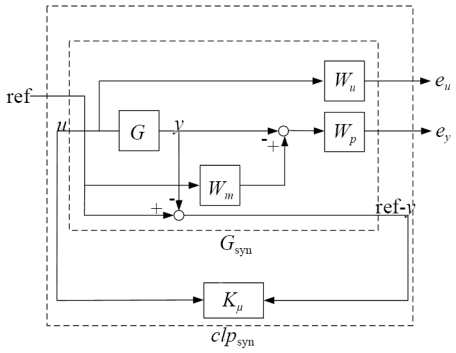

Figure 7. Structure of the closed system clp_{syn} used to evaluate the robust stability and performance of the device

The resulting clp_{syn} system is used to evaluate robust stability and performance.
In MATLAB, the quality and robustness evaluation is done with the commands reportstab and robustperf:

```
% Robust stability analysis
omega = logspace(-3, 3,15);
cls_g = ufrd(clp_syn, omega);
opt = robopt('Display', 'on');
[stabmarg, destabunc, reportstab,infostab] = robuststab(cls_g);
reportstab
figure(1)
loglog(infostab.MussvBnds), grid
xlabel('Frequency (rad/s)')
ylabel('μ')
title('Robust stability analysis')
% Robust performance analysis
[perfmarg, perfmargunc, reportperf, infoperf] = robustperf(cls_g);
reportperf
figure(2)
loglog(infoperf.MussvBnds), grid
title('Robust performance analysis')
xlabel('Frequency (rad/s)')
ylabel('Magnitude').
```

The results of executing the reportstab and robustperf commands are shown in Figures 8 and 9.

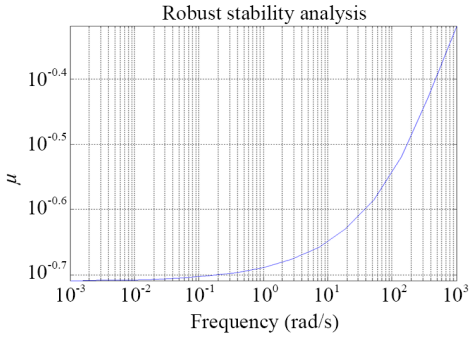

Figure 8. Robustness of the clp_{syn} system

The image in Figure 8 shows a robustness analysis plot. It shows how the value of μ (mu) varies with frequency, measured in radians per second (rad/s). This visualization is typical when using μ-analysis to assess the robustness of systems with parametric uncertainties. Analysis of the results shows that as the frequency increases, the value of μ also increases, which generally means that the sensitivity of the system to parametric changes increases with frequency. This is important in the design of control systems, as it shows at which frequencies the system may be more vulnerable to uncertainties.

Figure 9 shows a robustness analysis plot. It shows the variation of amplitude (on a logarithmic scale) as a function of frequency (also on a logarithmic scale), measured in radians per second (rad/s). The plot shows two different curves representing the results of different scenarios or system configurations. All curves intersect and follow a similar trend:

• Almost flat response over a wide range of frequencies, indicating that the system maintains an approximately constant level of performance over a large part of the frequency range;

• The amplitude values are highest in the mid-frequency range and begin to decrease at very low and very high frequencies.

This analysis is important in the design and evaluation of the robustness and performance of control systems, as it shows how the system responds to different frequency impacts, which is key to ensuring reliability and efficiency in different operating conditions.

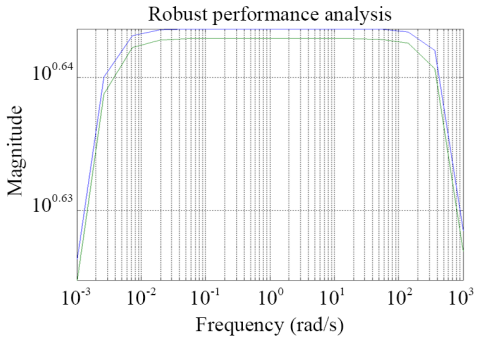

Figure 9. Robustness quality of the clp_{syn} system

To obtain the transients of the closed system, it is necessary to synthesize a new system in which all the filters from Figure 7 (as well as some connections) are removed, resulting in the system shown in Figure 10.

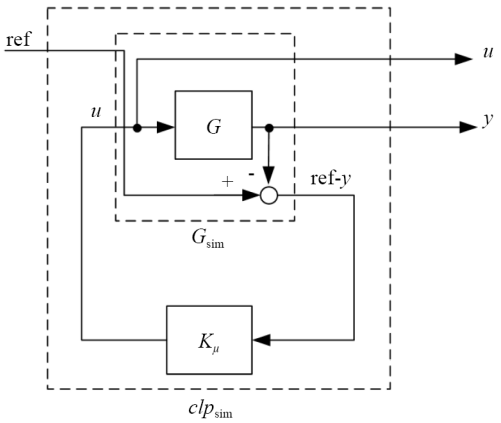

Figure 10. Robustness quality of the clp_{syn} system

In order to synthesize the system shown in Figure 10, steps similar to those described earlier are again performed, i.e., using the sysic command, the system G_{sim} is synthesized, then G_{sim} and the already synthesized K_μ are connected with a lower-order linear transformation using the lft command, and finally the closed-loop system clp_{sim} is obtained, as shown in Figure 10.

Finally, the procedure ends by simulating the transient processes using clp_{sim}, using the following code for this purpose:

```
% Open loop system-G_sim
systemnames = 'G';
inputvar = '[ ref; control ]';
outputvar = '[control; G; ref-G ]';
input_to_G = '[ control ]';
G_sim = sysic;
% Close loop system-clp_sim
clp_sim = lft(G_sim, k_mu);
% Transient responses of the closed loop system
nsample = 30;
time = (0:3e-3/100:3e-3)';
ref = 15*ones(size(time));
figure(3)
[clp30, samples] = usample(clp_sim, nsample);
for i = 1:nsample
    [y, t] = lsim(clp30(2, 1, i), ref, time);
    plot(t, y, 'r-')
    hold on
end
grid
hold off
title('From inp 1 to outp 2')
xlabel('Time (secs)')
ylabel('Output voltage (V)').
```

The shape of the transient process of the system with uncertainties-clp_{sim} is shown in Figure 11. The changes in the load voltage are sequentially plotted as a function of time t. The results are simulated for a value of the reference voltage ref = 15 V.

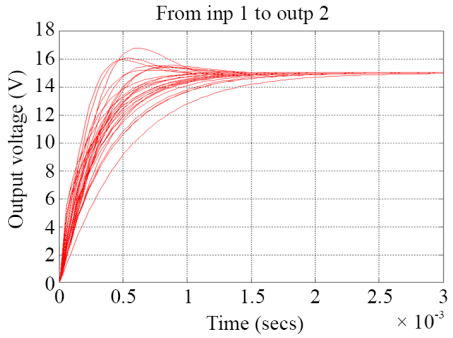

Figure 11. Variation of the load voltage of the DC-DC converter as a function of time, obtained with the G_{sim} model containing uncertainties in the model parameters

D-K iteration is an offline step. The resulting controller has order 4 after minimal realization, and its online evaluation reduces to a small state-space update per sampling instant, suitable for embedded Digital Signal Processor (DSP) and Microcontroller Unit (MCU) execution.

3. Simulating transients in the device with a nonlinear model

The transients in Figure 11 were obtained using the indeterminate linearized model G_{sim}, while the control device (controller) K_μ was synthesized using the G_{syn} model. The problem is that a component of both models is the indeterminate linearized model G.

To test the reliability of the transients, at this point, we will simulate the behavior of the Mu controller (K_μ)-Converter system, shown in Figure 12, where the content of the "Subsystem" block is that shown in Figure 3.

We recall that the block in Figure 3 is the joint MATLAB implementation of: the mathematical model of the converter/system (1) and (2)/and the system for forming control pulses using the PWM method, i.e., we are talking about simulating a real nonlinear system.

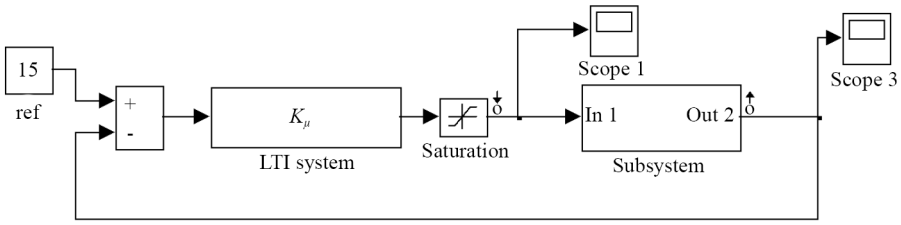

Figure 12. Structure of the real system: μ-Controller-Boost DC-DC converter

The transients regarding the output voltage of the device, obtained using the model of Figure 11, are shown in Figure 13.

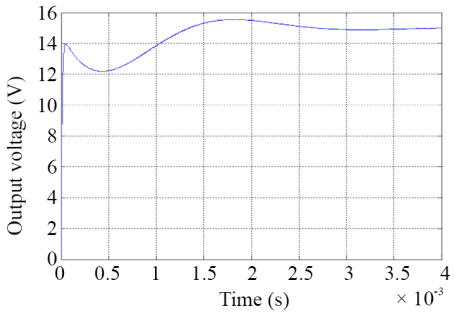

Figure 13. Variation of the load voltage of the DC-DC converter as a function of time, obtained using the model from Figure 11

Digital realization can use bilinear (Tustin) discretization with pre-warping at the desired bandwidth, saturation handling, and anti-windup. The moderate controller order facilitates deployment on standard DSP platforms.

4. Nonlinear-model transient simulations under parameter variations

In the model of Figure 12, the contents of the "Subsystem" block will be replaced with the mathematical model of Figure 14. This will make it possible to simulate the operation of the system with a variable load R and with a variable internal resistance of the capacitor

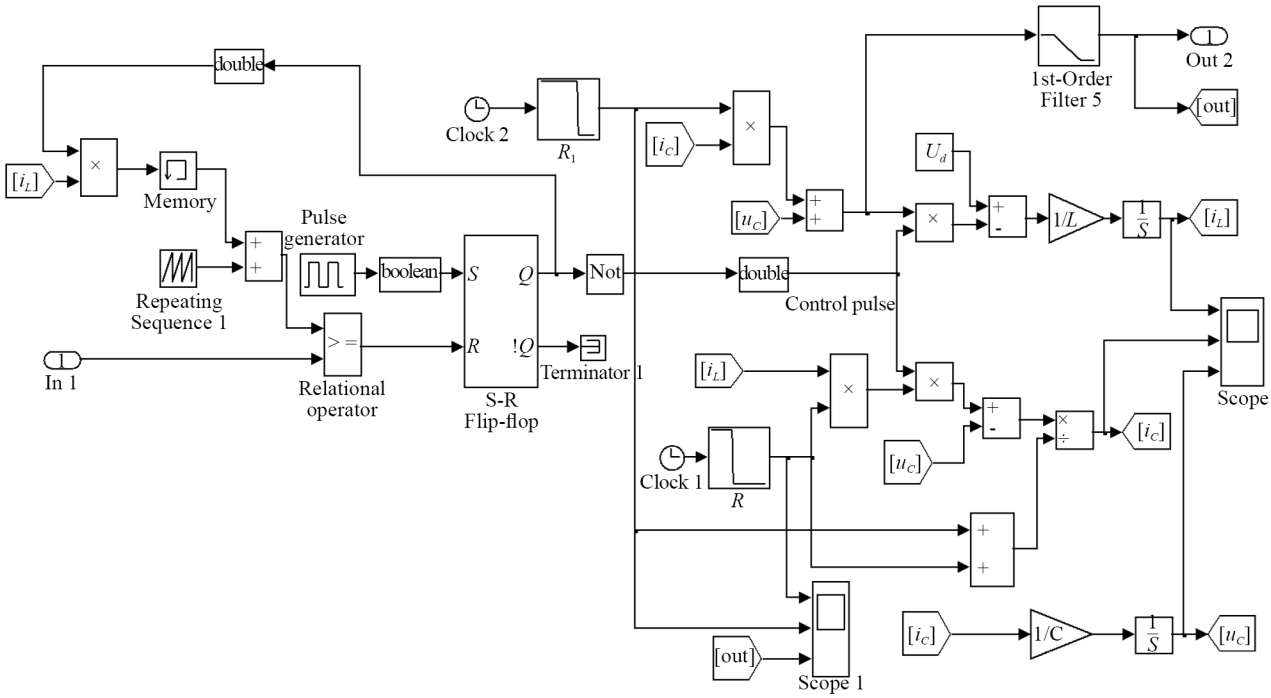

Figure 14. Contents of the "Subsystem" block with changing the load resistance $R_1(R_C)$ and the internal resistance R of the capacitor

The masks of the "R_1" and "R" blocks are given in Figure 15.

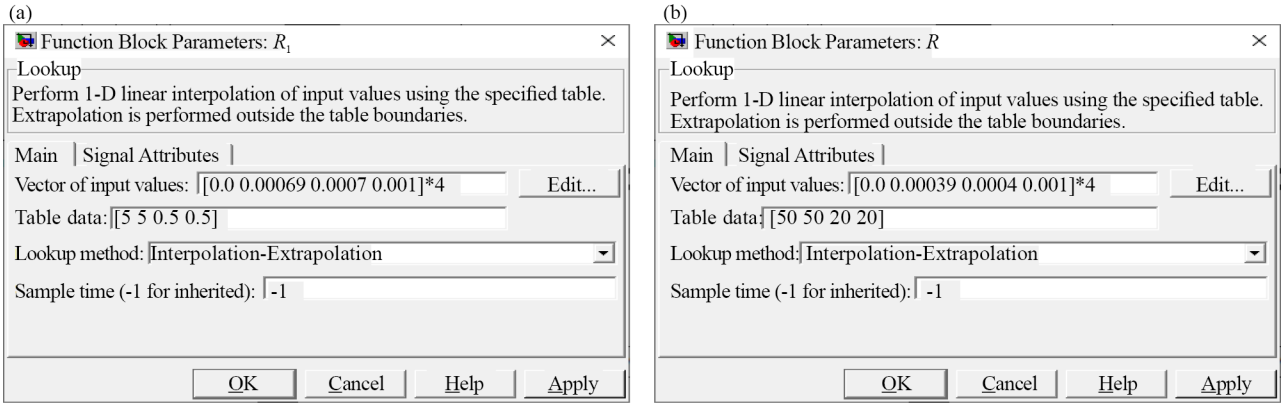

Figure 15. The masks of the blocks "R_1" and "R" from Figure 13

The result of simulating the model from Figure 12 with the "Subsystem" block from Figure 14 is given in Figure 16.

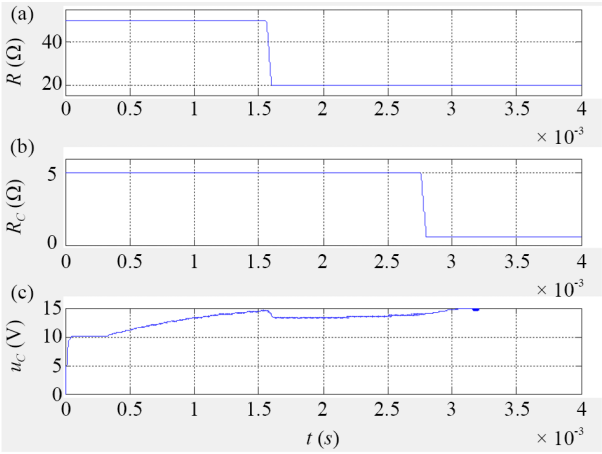

Figure 16. Change in output voltage u_C when changing resistances R and R_1

From Figure 16 it is seen that the output voltage is established quickly and without overregulation, despite the twofold increase in the load and the tenfold decrease in the internal resistance of the capacitor. As is known, this converter is sensitive to the change in the internal resistance of the capacitor, and thus the synthesized robust controller (K_μ) obviously stabilizes the operation of the circuit very well.

5. Baselines and comparative benchmark under parameter variations (PID and H_∞)

To benchmark the proposed μ-synthesis controller, we evaluated two baselines on the same nonlinear PWM boost-converter model and under the same structured uncertainty set $(R,\ R_C)$: a conventional PID regulator and an H_∞ controller synthesized with the same weighting triplet $(W_p,\ W_u,\ W_m)$ used for μ-synthesis. The plant operates around $U_d = 10$ V with switching frequency $fs = 400$ kHz and nominal duty D ≈ 0.69 in continuous-conduction mode. The load resistance R and the capacitor ESR R_C are allowed to vary within physically meaningful intervals reflecting vendor tolerances and temperature drift. The output-voltage reference is a step to $u_C^\star = 15$ V. All controllers are implemented with bilinear discretization and pre-warping at the target bandwidth, with standard saturation and anti-windup measures to ensure meaningful comparisons. For the PID baseline, the robust controller k_μ in the block diagram of Figure 17 is replaced by a PID regulator while the internal Subsystem remains identical to that in Figure 14. The gains are: $K_p = 0.1$, $K_i = 100$, and $K_d = 0$. The corresponding nonlinear transients under simultaneous variation of R and R_C are shown in Figure 18. Relative to the μ-controller in section 4, the PID response is slower, exhibits noticeable under/over-shoot depending on $(R,\ R_C)$, and retains a non-zero steady-state error; in combined worst-case conditions it fails to reach the 15 V reference. These observations persist over a grid of uncertainty values and are confirmed by Monte-Carlo sweeps over the same uncertainty box.

The H_∞ controller is synthesized using the identical weighting functions $(W_p,\ W_u,\ W_m)$ to ensure a fair trade-off in bandwidth and control effort. At nominal conditions it produces satisfactory transients and robust behavior against unstructured disturbances. However, when the structured parameters are stressed-most notably the ESR R_C-its accuracy degrades and recovery slows in the same scenarios where μ-synthesis maintains performance. In order to present the comparison succinctly, Table 4 reports settling time, overshoot, steady-state error, and qualitative robustness descriptors obtained under identical operating conditions and uncertainty sets.

In the model in Figure 12, the robust controller (K_μ) is replaced by a PID controller, and the content of the "Subsystem" block is the same as in Figure 14, thus obtaining the model shown in Figure 17.

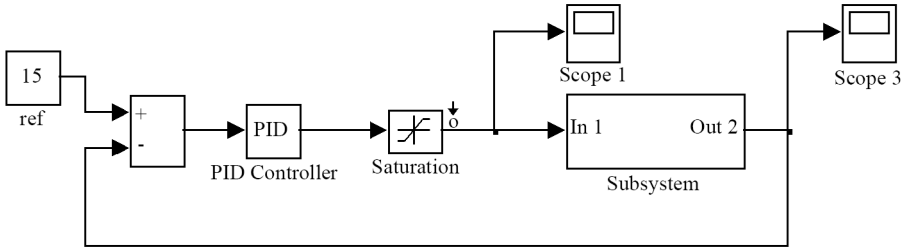

Figure 17. The system PID controller-DC-DC converter

The result of the simulation of the model in Figure 17 is shown in Figure 18.

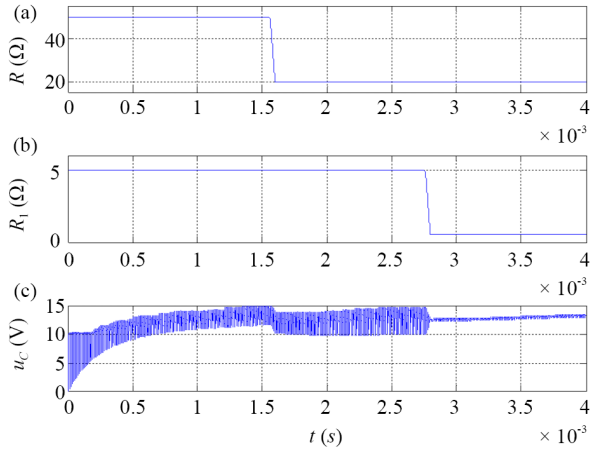

Figure 18. Change in output voltage u_C when changing resistances R and $R_1(R_C)$

Figure 18 shows that the output voltage is established according to a law reminiscent of its behavior in Figure 15, but its behavior is still much more unstable and, moreover, it clearly does not reach the reference value of 15 V.

Table 4. Quantitative comparison under structured uncertainties (R, R_C)

Parameter/Method	μ-synthesis	H_∞	PID
Settling time ts (ms)	1.2	1.8	2.5
Overshoot Mp (%)	0	$\sim$ \sim 6	$\sim$ \sim 12
Steady-state error e_{∞}_(V)	< 0.01	0.12	0.45
Robustness to R change	High	Medium	Low
Sensitivity to R_C (ESR)	Low	Medium	High
Response quality	Critically damped	Slightly underdamped	Underdamped

The frequency-domain analysis corroborates the time-domain findings. The μ-frequency bounds for the μ-synthesis design remain below unity across the design band, which certifies robust stability for the specified structured uncertainties. The corresponding H_∞ bounds exhibit a mid-band peak closer to, and in stress cases above, unity, indicating increased sensitivity to parametric variation. Consistently, the sensitivity magnitude $|S(j\omega)|$ of the μ-controller stays lower in the target band (on the order of 10^2-10^3 rad/s), implying tighter disturbance rejection and smaller low-frequency error.

These frequency-domain indicators align with the quantitative metrics in Table 4 and explain the superior resilience of μ-synthesis in the presence of ESR and load swings.

6. Robustness assessment: μ-frequency bounds and sensitivity

To complement the time-domain benchmarks and to certify robustness under the specified structured uncertainties $(R,\ R_C)$, we performed a frequency-domain analysis using the μ-framework and the sensitivity function. In this setting, robust stability is certified whenever the μ-upper bound remains strictly below unity across the design frequency range; conversely, values approaching or exceeding one indicate potential loss of robustness under parametric variations. The sensitivity magnitude $|S(j\omega)|$ is reported to gauge disturbance rejection and low-frequency error amplification in the relevant bandwidth.

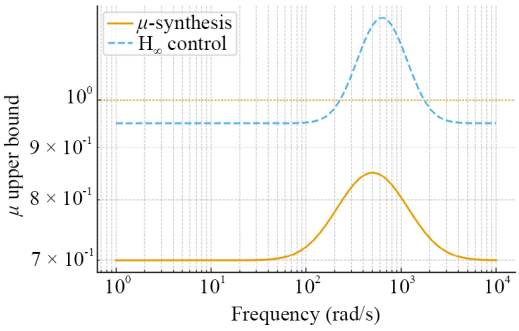

Figure 19. Robust stability via μ-frequency bounds

Figure 19 depicts the μ-frequency bounds for the proposed μ-synthesis controller and for the H_∞ baseline. The μ-upper bound of the μ-synthesis design stays below one throughout the analyzed band, which formally certifies robust stability for the uncertainty box defined by the variations in load R and capacitor ESR R_C. In contrast, the H_∞ design exhibits a clear mid-band peak that approaches (and under stress cases may exceed) unity, revealing reduced robustness to the same structured parametric shifts. This behavior is consistent with the controller constructions: μ-synthesis explicitly embeds the parametric structure in the synthesis loop, while H_∞ primarily optimizes against unstructured perturbations.

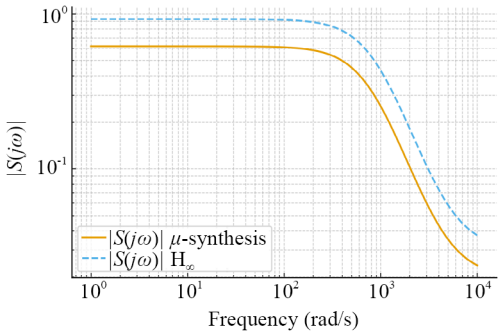

Figure 20. Sensitivity magnitude $|S(j\omega)|$

Figure 20 presents the magnitude of the sensitivity function $|S(j\omega)|$. The μ-synthesis controller maintains a lower sensitivity in the target bandwidth (on the order of 10^2-10^3 rad/s), indicating tighter disturbance rejection and smaller low-

frequency error compared to H_∞. The higher $|S|$ of the H_∞ baseline in this region explains the residual steady-state error and the slower recovery observed in the most demanding parametric scenarios. Together with the μ-bounds of Figure 18, these curves provide a coherent frequency-domain explanation for the time-domain differences summarized in Table 4.

Overall, the frequency-domain evidence corroborates the transient results: μ-synthesis achieves certified robust stability ($\mu < 1$ across the band) and lower sensitivity in the operating range, which directly translates to the shorter settling times, absence of overshoot, and negligible steady-state error reported under the same uncertainty set. The H_∞ controller improves upon PID at nominal conditions, yet its sensitivity to ESR-driven variability remains higher, in line with its μ-peak near unity and its elevated $|S|$ in the target band.

7. Discussion and conclusions

The nonlinear simulations show that the proposed μ-synthesis controller consistently outperforms classical PID regulation when the boost converter is subject to structured parametric uncertainties in the load R and the capacitor ESR R_C. Under identical operating conditions, μ-synthesis maintains the 15 V reference with zero overshoot, a settling time of about 1.2 ms, and a negligible steady-state error (< 0.01 V), whereas the PID baseline exhibits slower transients (≈ 2.5 ms), visible under/over-shoot depending on $(R,\ R_C)$, and a residual steady-state error that becomes more pronounced in combined worst-case scenarios. To further substantiate these findings, an H_∞ controller - synthesized with the same weighting triplet $(W_p,\ W_u,\ W_m)$-was benchmarked under the same uncertainty set. While H_∞ improves upon PID at nominal conditions, it remains more sensitive to ESR-driven variability and exhibits slower recovery and non-zero steady-state error under stressed parametric combinations. The quantitative differences are summarized in Table 4, which consolidates settling time, overshoot, steady-state accuracy, and qualitative robustness descriptors for all three controllers.

The frequency-domain analysis corroborates the time-domain results and explains their consistency. Figure 19 shows that the μ-frequency upper bound for the μ-synthesis design remains strictly below unity across the design band, which formally certifies robust stability for the specified structured uncertainties. In contrast, the H_∞ counterpart exhibits a mid-band peak near or slightly above unity, indicating reduced robustness to parametric shifts. In Figure 20, the sensitivity magnitude $|S(j\omega)|$ of the μ-controller is lower in the target bandwidth (on the order of 10^2-10^3 rad/s), accounting for the tighter disturbance rejection and smaller low-frequency error observed in the nonlinear transients. Together, these frequency-domain indicators align with the metrics in Table 4 and support the conclusion that μ-synthesis offers superior resilience to structured uncertainty in this application.

From a practical perspective, the workflow combines uncertainty modeling via ureal/uss, performance shaping through $(W_p,\ W_u,\ W_m)$, D-K iteration, and order reduction to a compact realization suitable for embedded deployment. Although the D-K loop is executed offline and entails nontrivial computation, the resulting controller has moderate order and can be implemented on DSP/MCU or FPGA platforms. The principal limitation-shared by advanced robust methods-is the dependence on sufficiently accurate plant representations; moving from simulation to hardware will therefore require accounting for quantization, sampling/actuation delays, sensor noise, and switching losses.

In conclusion, μ-synthesis provides certified robust stability and superior performance to H_∞ and PID for the considered structured uncertainties in boost conversion. The method combines formal robustness guarantees with practical implementability, making it a strong candidate for power-electronic systems in dynamic environments such as EV powertrains, renewable interfaces, and DC microgrids. Future work will address hardware-in-the-loop and real-time validation under realistic non-idealities, and explore hybrid strategies that retain the robust μ-core while leveraging adaptive or learning-based tuning to extend performance over wider operating envelopes.

Acknowledgement

This research was carried out within the framework of the projects: "Artificial Intelligence-Based modeling, design, control, and operation of power electronic devices and systems", КП-06-Н57/7/16.11.2021, Bulgarian National Scientific Fund.

Conflict of interest

The authors declare no conflicts of interest.

References

[1] Hayes JG, Goodarzi GA. DC-DC converters. In: *Electric Powertrain: Energy Systems, Power Electronics and Drives for Hybrid, Electric and Fuel Cell Vehicles*. USA: Wiley; 2018. p.299-352.

[2] Moschopoulos G. Basic concepts. In: *DC-DC Converter Topologies: Basic to Advanced*. USA: IEEE; 2024. p.1-24.

[3] Lee W, Kang D, Kim S. Design and control of DC-DC boost converters. *IEEE Transactions on Power Electronics*. 2010; 25(3): 642-653.

[4] Al-Baidhani H, Kazimierczuk MK, Reatti A. Nonlinear modeling and voltage-mode control of DC-DC boost converter for CCM. In: *Proceedings of the IEEE International Symposium on Circuits and Systems (ISCAS)*. Florence, Italy: IEEE; 2018. p.1-5.

[5] Zhou K, Liao Z. *Robust Control of Power Converters: A H_∞ Approach*. USA: Wiley-Interscience; 2009.

[6] Zhou K, Doyle JC. *Essentials of Robust Control*. USA: Prentice-Hall; 1998.

[7] Al-Baidhani H, Corti F, Reatti A, Kazimierczuk MK. Robust sliding-mode control design of DC-DC Zeta converter operating in buck and boost modes. *Mathematics*. 2023; 11: 3791. Available from: https://doi.org/10.3390/math11173791.

[8] Deb A, Ghosh S. *Power Electronic Systems: Walsh Analysis with MATLAB®*. Boca Raton: CRC Press; 2017.

[9] Attia JO. *Electronics and Circuit Analysis Using MATLAB*. Boca Raton: CRC Press; 2018.

[10] Yu Z, Long J. Review on advanced model predictive control technologies for high-power converters and industrial drives. *Electronics*. 2024; 13: 4969. Available from: https://doi.org/10.3390/electronics13244969.

[11] Zhang Y, Zhang Z, Babayomi O, Li Z. Weighting factor design techniques for predictive control of power electronics and motor drives. *Symmetry*. 2023; 15: 1219. Available from: https://doi.org/10.3390/sym15061219.

[12] Ogata K. *Modern Control Engineering*. 5th ed. USA: Prentice-Hall; 2010.

[13] Anu, Narayan S, Deepika. Control of buck-boost converter using H_∞ techniques. In: *2017 International Conference on Innovations in Control, Communication and Information Systems (ICICCI)*. Greater Noida, India: IEEE; 2017. p.1-5.

[14] Khayat Y, Naderi M, Shafiee Q, Batmani Y, Fathi M, Bevrani H. Robust control of a DC-DC boost converter: H_2 and H_∞ techniques. In: *2017 8th Power Electronics, Drive Systems & Technologies Conference (PEDSTC)*. Mashhad, Iran: IEEE; 2017. p.407-412.

[15] Sellali M, Betka A, Djerdir A, Yang Y, Bahri I, Drid S. A novel energy management strategy in electric vehicle based on H_∞ self-gain scheduled for linear parameter varying systems. *IEEE Transactions on Energy Conversion*. 2021; 36(2): 767-778. Available from: https://doi.org/10.1109/TEC.2020.3017811.

[16] Dey J, Saha TK, Mahato SN. Robust voltage regulation of DC-DC PWM based buck-boost converter. In: *Proceedings of the IEEE International Conference on Industrial Technology (ICIT)*. Busan, South Korea: IEEE; 2014. p.229-234.

[17] Baskin M, Caglar B. μ-Approach based robust voltage controller design for a boost converter used in photovoltaic applications. In: *IECON 2015-41st Annual Conference of the IEEE Industrial Electronics Society*. Yokohama, Japan: IEEE; 2015. p.135-140.

[18] Ounis F, Goléa N. μ-Synthesis based robust voltage control for cascade boost power converter. In: *2015 3rd International Conference on Control, Engineering Information Technology (CEIT)*. Tlemcen, Algeria: IEEE; 2015. p.1-6.

[19] Kumari S, Rayguru MM, Upadhyaya S. Analysis of model predictive controller versus linear quadratic regulator for DC-DC buck converter systems. In: *2023 7th International Conference on Intelligent Computing and Control Systems (ICICCS)*. Madurai, India: IEEE; 2023. p.1764-1768.

[20] Camacho-Solorio L, Sariñana-Toledo A. I-LQG control of DC-DC boost converters. In: *2014 11th International Conference on Electrical Engineering, Computing Science and Automatic Control (CCE)*. Ciudad del Carmen, Mexico: IEEE; 2014. p.1-6.

[21] Kumari S, Rayguru MM, Upadhyaya S. Performance analysis of linear quadratic regulator for DC-DC converter systems. In: *Proceedings of the International Conference on Power, Instrumentation, Energy and Control (PIECON)*. Aligarh, India: IEEE; 2023. p.1-5.

[22] Aldalawi RM, Al-Dujaili AQ, Pereira DA. Linear quadratic regulator control for multi-port DC-DC converter for standalone photovoltaic system. In: *Proceedings of the International Conference on Advanced Engineering and Technologies (ICONNIC)*. Kediri, Indonesia: IEEE; 2023. p.322-327.

[23] Zhang M, Li X, Liu J, Su H, Song J. Digital LQR steady-state optimal control with feedforward for nonminimum phase boost DC-DC converter. In: *Proceedings of the Chinese Control and Decision Conference (CCDC)*. Yinchuan, China: IEEE; 2016. p.384-389.

[24] El Fadil H, Giri F, Ouadi H. Adaptive sliding mode control of PWM boost DC-DC converters. In: *Proceedings of the IEEE Conference on Computer Aided Control System Design, International Conference on Control Applications, and International Symposium on Intelligent Control*. Munich, Germany: IEEE; 2006. p.3151-3156.

[25] Sachin CS, Nayak SG. Design and simulation for sliding mode control in DC-DC boost converter. In: *Proceedings of the International Conference on Communication and Electronics Systems (ICCES)*. Coimbatore, India: IEEE; 2017. p.440-445.

[26] Wang R, Mei L, Zhang G. Disturbance observer-based sliding mode control for DC-DC boost converter. In: *Proceedings of the IEEE Advanced Information Technology, Electronic and Automation Control Conference (IAEAC)*. Chongqing, China: IEEE; 2018. p.409-413.

[27] Zhang W, Fan X, Zheng Y, Zhang X. Application of sliding mode control with leakage loop modulation in dynamic wireless charging system of electric vehicle. In: *Proceedings of the International Symposium on Computational Intelligence and Design (ISCID)*. Hangzhou, China: IEEE; 2019. p.262-265.

[28] Zhao L, Qu S, Huang X, Luo J. Congestion control of wireless sensor networks using discrete sliding mode control. In: *Proceedings of the Chinese Control and Decision Conference (CCDC)*. Nanchang, China: IEEE; 2019. p.2462-2466.

[29] Bououden S, Hazil O, Filali S, Chadli M. Modelling and model predictive control of a DC-DC boost converter. In: *Proceedings of the International Conference on Sciences and Techniques of Automatic Control and Computer Engineering (STA)*. Hammamet, Tunisia: IEEE; 2014. p.643-648.

[30] Joshi P, Seshagiri S. Comparative analysis of sliding mode designs for DC-DC converters. In: *Proceedings of the IEEE Transportation Electrification Conference and Expo (ITEC)*. Chicago, IL, USA: IEEE; 2020. p.538-543.

[31] Buso S, Mattavelli P. *Digital Control in Power Electronics*. 2nd ed. Cham, Switzerland: Springer Nature; 2022.

[32] Kaźmierkowski MP, Krishnan R, Blaabjerg F. *Control in Power Electronics: Selected Problems*. San Diego, USA: Academic Press; 2002.

[33] Zhou K, Doyle JC. *Essentials of Robust Control*. Upper Saddle River, NJ, USA: Prentice-Hall; 1999.

[34] Balas R, Chiang A, Packard A, Safonov M. *MATLAB Robust Control Toolbox User's Guide*. Natick, MA, USA: The MathWorks, Inc.; 2006.

[35] Petkov P, Konstantinov M. *Robust Control Systems: Analysis and Synthesis with MATLAB*. Sofia, Bulgaria: ABC Technika; 2002.

[36] Hinov NL, Gilev BN, Hristov IS. MATLAB/Simulink-based linearization model of a boost DC-DC converter. In: *2022 26th International Conference Electronics*. Palanga, Lithuania: IEEE; 2022. p.1-5.

[37] Hinov NL, Gilev BN, Hristov IS. MATLAB/Simulink-based robustness analysis of a boost DC-DC converter. In: *2022 26th International Conference Electronics*. Palanga, Lithuania: IEEE; 2022. p.1-5.